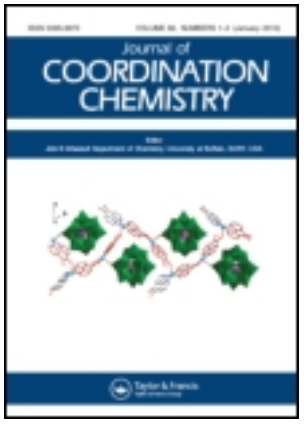

Journal of Coordination Chemistry
Publication details, including instructions for authors and subscription information:
http://www.tandfonline.com/loi/gcoo20

Synthesis and structure of a new tetracopper(II) complex with N-benzoate-N′-[2-(2-hydroxyethylamino)ethyl]oxamide as bridging ligand: in vitro anticancer activities and DNA- and BSA-binding studies

Ting-Ting Xing[a], Shu-Hui Zhan[b], Yan-Tuan Li[a], Zhi-Yong Wu[a] & Cui-Wei Yan[c]

[a] Marine Drug and Food Institute, Ocean University of China, Qingdao, P.R. China.

[b] Qingdao Municipal Medical Group, Qingdao, P.R. China.

[c] College of Marine Life Science, Ocean University of China, Qingdao, P.R. China.

Accepted author version posted online: 23 Jul 2013.Published online: 24 Sep 2013.

To cite this article: Ting-Ting Xing, Shu-Hui Zhan, Yan-Tuan Li, Zhi-Yong Wu & Cui-Wei Yan (2013) Synthesis and structure of a new tetracopper(II) complex with N-benzoate-N′-[2-(2-hydroxyethylamino)ethyl]oxamide as bridging ligand: in vitro anticancer activities and DNA- and BSA-binding studies, Journal of Coordination Chemistry, 66:18, 3149-3169, DOI: 10.1080/00958972.2013.827179

To link to this article: http://dx.doi.org/10.1080/00958972.2013.827179

Journal of Coordination Chemistry, 2013
Vol. 66, No. 18, 3149–3169, http://dx.doi.org/10.1080/00958972.2013.827179

Synthesis and structure of a new tetracopper(II) complex with *N*-benzoate-*N*′-[2-(2-hydroxyethylamino)ethyl]oxamide as bridging ligand: *in vitro* anticancer activities and DNA- and BSA-binding studies

TING-TING XING†, SHU-HUI ZHAN‡, YAN-TUAN LI*†, ZHI-YONG WU† and CUI-WEI YAN*§

†Marine Drug and Food Institute, Ocean University of China, Qingdao, P.R. China
‡Qingdao Municipal Medical Group, Qingdao, P.R. China
§College of Marine Life Science, Ocean University of China, Qingdao, P.R. China

(*Received 4 March 2013; in final form 12 July 2013*)

A new tetracopper(II) complex bridged by oxamido and carboxylate, $[Cu_4(bhyox)_2(phen)_2(H_2O)_2](pic)_2$, where H_3bhyox, phen and Hpic denote *N*-benzoate-*N*′-[2-(2-hydroxyethylamino)ethyl]oxamide, 1,10-phenanthroline, and 2,4,6-trinitrophenol, respectively, has been synthesized and characterized by elemental analysis, molar conductivity, IR, electronic spectra, and single-crystal X-ray diffraction. The crystal structure reveals that the cyclic tetracopper(II) cation $[Cu_4(bhyox)_2(phen)_2(H_2O)_2]^{2+}$ with an embedded center of inversion is assembled by a pair of *cis*-oxamido-bridged bicopper(II) units via carboxylate bridges, in which copper(II) ions are distorted square pyramidal. The Cu···Cu separations through the oxamido and the carboxylate bridges are 5.1944 (6) and 5.3344(7) Å, respectively. In the crystal, the supramolecular structure is composed of classical hydrogen bonding chains assembled by 2D non-classical hydrogen-bonding networks and π–π stacking interaction. *In vitro* cytotoxicity experiment shows that the tetracopper(II) complex exhibits cytotoxic activity against the SMMC7721 and A549 cell lines. The reactivity towards herring sperm DNA (*HS*-DNA) and protein bovine serum albumin (BSA) suggests that the tetracopper(II) complex can interact with the DNA by intercalation, and the complex binds to protein BSA responsible for quenching of tryptophan fluorescence by static quenching mechanism.

Keywords: Crystal structure; Tetracopper(II) complex; μ-Oxamidato-bridge; DNA interaction; BSA binding

1. Introduction

Synthesis and reactivities of metal complexes toward DNA and protein have been active fields of research for gaining insight into the reactive models for protein–nucleic acid interactions, as probes of DNA structure for biochemical procedures governing protein sequencing, footprinting and folding studies, and for obtaining the information about drug design and tools of molecular biology [1–3]. *Cis*-platin and related platinum-based drugs are among the most widely used antitumor metallodrugs for the treatment of certain human

*Corresponding authors. Email: yantuanli@ouc.edu.cn (Y.-T. Li); cuiweiyan@ouc.edu.cn (C.-W. Yan)

cancers with incredible success, but the severe toxic side effects limit their potential [4, 5]. DNA is the pharmacological target of *cis*-platin and related platinum-based drugs with platinum forming covalent bonds to N7 of adjacent purine bases for cytotoxic activity [6, 7]. Therefore, the design and synthesis of new metal-based anticancer drugs that exhibit less toxicity, enhanced selectivity, and non-covalent DNA binding are of interest [8]. The non-covalent DNA interactions include intercalative, electrostatic, and groove binding. Intercalation strongly affects the properties of DNA and has been reported as a preliminary step in mutagenesis [9]. Intercalating ability relates with the planarity of ligands, the coordination geometry of the metal ion, and donor type of the ligand. Metal ion types and valence play important roles in deciding the binding to DNA.

Proteins are important chemical substances and major targets for many types of medicines. Studies on binding of metal complexes with protein also interpret the metabolism and transporting process. Serum albumins, the most abundant protein in the blood circulatory system, play important roles in transport and deposition of a variety of exogenous compounds [10]. Among the serum albumins, bovine serum albumin (BSA) has been studied extensively, partly due to its structural homology with human serum albumin, its availability, low cost, and unusual ligand binding properties [11]. Thus, the reactivities of metal complexes toward DNA and protein BSA are important in understanding the mechanism of binding and in the rational design of metallodrugs [11].

Many investigations of reactivities of transition metal complexes with DNA and protein have focused on the selection of metal ions and the design of ligands. Consequently, new DNA- and BSA-targeted drugs are based on different transition metal ions. Copper, as a biologically active metal element, has many correlations with endogenous oxidative deoxyribonucleic acid damage associated with aging and cancer, and its complexes are known to exhibit antitumor activity [12, 13]. Particularly, copper complexes containing heterocyclic bases have been extensively explored [14, 15], since Sigman *et al*. discovered that copper ion coordinated to 1,10-phenanthroline (phen) can cleave DNA [16]. Compared to mono- and bicopper(II) complexes [17], relatively few studies on tetracopper(II) complexes have been reported [18]. However, enhancement of DNA-binding activity for tetranuclear complexes [19] together with the fact that relatively few reactivities of tetranuclear complexes toward protein has been investigated [20, 21], stimulates us to design and synthesize new tetracopper(II) complexes. In the context of design and synthesis of polynuclear complexes, it is generally known that *N*,*N*′-bis(substituted)oxamides could be good bridging ligand candidates because their coordinating abilities toward transition metal ions can be modified and tuned by changing the nature of the amide substituents [22, 23]. Many oxamido-bridged polynuclear complexes with symmetric *N*,*N*′-bis(substituted)oxamide ligands have been prepared, while only a few asymmetric *N*,*N*′-bis(substituted)oxamide polynuclear complexes have been reported because of the difficulties in their synthesis [24]. Exploration of the interactions of these complexes with DNA and protein BSA encourages us to design and synthesize new tetracopper(II) complexes with asymmetric *N*,*N*′-bis (substituted)oxamide as bridges to get an insight into the reactivity of such complexes toward DNA and protein BSA.

Recently, we reported the structure and DNA-binding properties of a tetracopper(II) complex with *N*-benzoate-*N*′-[2-(2-hydroxyethylamino)ethyl]oxamide (H_3bhyox) as bridging ligand and end-capping with 2,2′-diamino-4,4′-bithiazole (dabt) [25]. In order to evaluate the influence of different terminal ligands in tetracopper(II) complexes on structure, DNA-binding properties and cytotoxic activities, and to gain insight into the reactivity of this kind of complexes towards protein BSA. In this paper, we describe the synthesis and structure of

a new tetracopper(II) complex $[Cu_4(bhyox)_2(phen)_2(H_2O)_2](pic)_2$. *In vitro* cytotoxic activities and the reactivities of the tetracopper(II) complex toward herring sperm DNA *(HS*-DNA*)* and BSA are also reported. The results suggest that different terminal ligands in tetranuclear complexes may play an important role in DNA- and BSA-binding properties and cytotoxic activities.

2. Experimental

2.1. *Materials and chemicals*

The bridging ligand *N*-benzoate-*N′*-[2-(2-hydroxyethylamino)ethyl]oxamide (H_3bhyox) was synthesized according to literature method [25]. *HS*-DNA, ethidium bromide (EB), and BSA were purchased from Sigma Corp. and used as supplied. All other chemical reagents were of AR grade and obtained commercially.

2.2. *Physical measurements*

Carbon, hydrogen, and nitrogen elemental analysis were carried out with a 240-Perkin–Elmer elemental analyzer. Molar conductance was measured with a Shanghai DDS-11A conductometer. The infrared spectrum was recorded as KBr pellets in a Nicolet 470 spectrophotometer from 4000 to 400 cm^{-1}. The UV–visible spectrum was recorded in a 1 cm path length quartz cell on a Cary 300 spectrophotometer. Fluorescence was tested on an Fp-750w fluorometer equipped with quartz cuvettes of 1 cm path length. A CHI 832 electrochemical analyzer (Shanghai CHI Instrument, Shanghai, China) with a glassy carbon working electrode (GCE), a saturated calomel reference electrode, and a platinum wire counter electrode was used for electrochemical measurements. The GCE surface was freshly polished to a mirror prior to each experiment with 0.05 μm α-Al_2O_3 paste and then cleaned with water for 5 min. Viscosity measurement was carried out using an Ubbelohde viscometer immersed in a thermostatic water bath maintained at 289 (±0.1) K.

2.3. *Synthesis of $[Cu_4(bhyox)_2(phen)_2(H_2O)_2](pic)_2$*

To a stirred ethanol solution (5 mL) containing $Cu(pic)_2 \cdot 6H_2O$ (0.0627 g, 0.1 mM) was added an ethanol solution (10 mL) of H_3bhyox (0.0148 g, 0.05 mM) and piperidine (0.0128 g, 0.15 mM) at room temperature. After stirring for 30 min, an ethanol solution (5 mL) of phen (0.0099 g, 0.05 mM) was added dropwise and a small amount of pale yellow precipitate (containing [pipH](pic)) formed. The mixture was continually stirred at 333 K for 6 h, and then the precipitate obtained was filtered. Yellow green cube crystals of the complex suitable for X-ray analysis were obtained from the above filtrate by slow evaporation at room temperature after 15 days. Yield: 0.0659 g (78%). Anal. Calcd for $Cu_4C_{62}H_{52}N_{16}O_{26}$ (%): C, 44.03; H, 3.10; N, 13.25. Found (%): C, 43.97; H, 3.08; N, 13.32.

2.4. *Determination of X-ray crystal structure*

X-ray diffraction for the tetracopper(II) complex was made on a Bruker APEX area-detector diffractometer with graphite monochromated Mo-Kα radiation ($\lambda = 0.71073$ Å). The crystal structure was solved by direct methods followed by Fourier synthesis. Structure

refinements were performed by full-matrix least-squares procedures using SHELXL-97 on F^2 [26]. Hydrogens on O and N were found in a difference Fourier map and refined freely except for O–H distances restrained to 0.82 (hydroxyl) and 0.86 Å (water). All hydrogens on carbon were placed in calculated positions, with C–H = 0.97 (methylene) and 0.93 Å (aromatic), then refined in riding mode, with Uiso(H) = 1.2 Ueq(C). Crystal data and structural refinement parameters are summarized in table 1 and selected bond distances and angles are listed in table 2.

2.5. In vitro *cytotoxic activity evaluation by sulforhodamine B assays*

In vitro cytotoxic activities of the tetracopper(II) complex were evaluated against two cancer cell lines including SMMC-7721 and A549 by using the sulforhodamine B (SRB) assay. All cells were cultured in RPMI 1640 supplemented with 10% (v/v) fetal bovine serum, 1% (w/v) penicillin (104 U mL^{-1}), and 10 mg mL^{-1} streptomycin. Cell lines were maintained at 310 K in a 5% (v/v) CO_2 atmosphere with 95% (v/v) humidity. Cultures were passaged weekly using trypsine-EDTA to detach the cells from their culture flasks. The tetracopper(II) complex was dissolved in DMSO and diluted to the required concentration with the culture medium. The content of DMSO in the final concentration did not exceed 0.1%. At this concentration, DMSO was nontoxic to the cells tested. Rapidly growing cells were harvested, counted, and incubated at the appropriate concentration in 96-well microplates for 24 h. The tetracopper(II) complex dissolved in culture medium was then applied to the culture wells to achieve final concentrations from 10^{-4} to 10^{-1} μM. Control wells were prepared by the addition of culture medium without cells. The plates were incubated at 310 K in a 5% CO_2 atmosphere for 48 h. Upon completion of the incubation, the cells were fixed with ice-cold 10% trichloroacetic acid (100 mL) for 1 h at 277 K, washed five times in distilled water and allowed to dry in air and stained with 0.4% SRB in 1% acetic acid (100 mL) for 15 min. The cells were washed four times in

Table 1. Crystal data for $[Cu_4(bhyox)_2(phen)_2(H_2O)_2](pic)_2$.

Formula	$C_{62}H_{52}Cu_4N_{16}O_{26}$
Formula weight	1691.36
Crystal system	Triclinic
Space group	*P-1*
a (Å)	9.7438(12)
b (Å)	11.5695(14)
c (Å)	15.0256(18)
α (°)	97.128(2)
β (°)	102.648(2)
γ (°)	98.478(2)
V (Å^3)	1613.1(3)
D(Calcd) [g cm^{-3}]	1.741
Z	1
μ (Mo Kα) (mm^{-1})	1.403
F(0 0 0)	860
Crystal size (mm)	0.20 × 0.22 × 0.25
Temperature (K)	296
Radiation (Å)	Mo Kα 0.71073
θ range	1.80–25.23
Tot., Uniq. data, R(int)	8044, 5767, 0.0138
Observed data [$I > 2\sigma(I)$]	4845
R, ωR_2, S	0.0316, 0.0887, 1.036
Max., av. shift/error	0.000, 0.000

Table 2. Selected bond distances (Å) and angles (°).

Bond distances (Å)			
Cu1–O1	1.8932(17)	Cu1–O6	2.442(2)
Cu1–N1	1.9944(19)	Cu1–N2	1.906(2)
Cu1–N3	2.080(2)	Cu2–O2^{i}	2.3327(19)
Cu2–O3	1.9675(17)	Cu2–O4	1.9271(17)
Cu2–N4	1.992(2)	Cu2–N5	1.978(2)
C8–O3	1.271(3)	C8–N1	1.305(3)
C9–O4	1.271(3)	C9–N2	1.279(3)
Bond angles (°)			
O1–Cu1–O6	97.54(7)	O1–Cu1–N1	93.86(7)
O1–Cu1–N2	167.04(9)	O1–Cu1–N3	99.45(8)
O6–Cu1–N1	94.62(7)	O6–Cu1–N2	95.39(8)
O6–Cu1–N3	89.25(8)	N1–Cu1–N2	84.17(8)
N1–Cu1–N3	165.54(8)	N2–Cu1–N3	81.60(9)
O2^{i}–Cu2–O3	88.77(7)	O2^{i}–Cu2–O4	101.15(7)
O3–Cu2–O4	85.15(7)	O2^{i}–Cu2–N4	95.37(8)
O2^{i}–Cu2–N5	98.27(7)	O3–Cu2–N4	97.50(8)
O3–Cu2–N5	172.90(8)	O4–Cu2–N4	163.32(8)
O4–Cu2–N5	92.57(8)	N4–Cu2–N5	82.79(8)

Note: Symmetry codes: (i) 1−x, −y, 1−z.

1% acetic acid and air dried. The stain was solubilized in 10 mM unbuffered Tris base (100 mL) and the OD of each well was measured at 540 nm on a microplate spectrophotometer. The IC_{50} value was calculated from the curve constructed by plotting cell survival (%) *versus* the tetracopper(II) complex concentration.

2.6. *DNA-binding studies*

All experiments involving *HS*-DNA were performed in tris(hydroxymethyl)aminomethane-HCl (Tris-HCl) buffer solution (pH 7.14), which was prepared using deionized and sonicated triply distilled water. Solution of DNA in Tris-HCl buffer gave the ratio of UV absorbance at 260 and 280 nm, A_{260}/A_{280}, of *ca.* 1.9, indicating that the DNA was sufficiently free of protein [27]. The concentration of the prepared DNA stock solution was determined according to its absorbance at 260 nm. The molar absorption coefficient, ε_{260}, was taken as 6600 $M^{-1}\,cm^{-1}$ [28]. Stock solution of DNA was stored at 277 K and used after no more than four days. Concentrated stock solution of the tetracopper(II) complex was prepared by dissolving the complex in DMSO and diluted with Tris-HCl buffer to required concentrations for all the experiments. Absorption spectral titration was performed by keeping the concentration of the tetracopper(II) complex constant while varying the *HS*-DNA concentration. Equal solution of *HS*-DNA was added to the tetracopper(II) complex solution and reference solution to eliminate the absorbance of *HS*-DNA itself. In EB fluorescence displacement experiment, 5 μL of the EB Tris-HCl solution (1 mM) was added to 1 mL of *HS*-DNA solution (at saturated binding levels) [29] and stored in the dark for 2 h. Then, the solution of the tetracopper(II) complex was titrated into the DNA/EB mixture and diluted in Tris-HCl buffer to 5 mL. Before measurements, the mixture was shaken and incubated at room temperature for 30 min. The fluorescence spectra of EB bound to *HS*-DNA were obtained at an emission wavelength of 584 nm in the fluorometer keeping the concentration of *HS*-DNA constant, while varying the concentration of the tetracopper(II) complex. Electrochemical titration was performed by keeping the

concentration of the tetracopper(II) complex constant, while varying the *HS*-DNA concentration using the solvent of 50 mM NaCl/5 mM Tris-HCl buffer solution at pH 7.16. All voltammetric experiments were performed in a single compartment cell. The supporting electrolyte was 50 mM NaCl/5 mM Tris-HCl buffer solution at pH 7.16. Solutions were deoxygenated by purging with nitrogen for 15 min prior to measurements; during measurements a stream of N_2 was passed over the solution. In viscosity measurement, *HS*-DNA sample approximately, 200 base pairs in length, was prepared by sonication in order to minimize the complexities arising from DNA flexibility [30]. Flow times were measured with a digital stopwatch, each sample measured three times, and an average flow time was calculated. Relative viscosities for *HS*-DNA in the presence and absence of the tetracopper (II) complex were calculated from the relation $\eta = (t - t_0)/t_0$, where t is the observed flow time of DNA-containing solution and t_0 is that of Tris-HCl buffer alone. Data were presented as $(\eta/\eta_0)^{1/3}$ *versus* binding ratio [31], where η is the viscosity of DNA in the presence of tetracopper(II) complex and η_0 is the viscosity of DNA alone.

2.7. *BSA interaction studies*

All experiments involving BSA were performed in 50 mM NaCl/Tris-HCl buffer solution (pH 7.14). Solutions of BSA and the tetracopper(II) complex were prepared by dissolving them in NaCl/Tris-HCl buffer solution to the required concentrations. For UV absorption, a 5 mL solution of BSA (10 μM) was titrated with various concentrations of the complex. Equal solutions of complex were added to the reference solutions to eliminate the absorbance of the tetracopper(II) complex itself. In the tryptophan fluorescence quenching experiment, quenching of the tryptophan residues of BSA [32] was done by keeping the concentration of BSA constant while varying the tetracopper(II) complex (quencher) concentration, producing solutions with varied mole ratio of the quenchers to BSA. The fluorescence spectra were recorded at an excitation wavelength of 295 nm and an emission wavelength of 347 nm in a fluorometer after each addition of the quencher.

3. Results and discussion

3.1. *Synthesis and general properties of the tetracopper(II) complex*

Our aim of this study was to obtain tetracopper(II) complex with asymmetric *N*,*N*′-bis (substituted)oxamide as bridging ligand. Therefore, *N*-benzoate-*N*′-[2-(2-hydroxyethylamino)ethyl]oxamide (H_3bhyox), which can coordinate to the metal ions through carbonyl oxygens, nitrogens of oxamido, and oxygens of carboxyl [25], was chosen as a bridging ligand; 1,10-phenanthroline (phen) was used as the terminal ligand. In the course of preparing the complex, piperidine as base makes H_3bhyox coordinate to copper(II) through deprotonated oxamido nitrogen and carboxyl oxygen. Elemental analysis indicate that the reaction of H_3bhyox with $Cu(pic)_2 \cdot 6H_2O$ and phen in 1 : 2 : 1 mole ratio yielded $[Cu_4(bhyox)_2(phen)_2(H_2O)_2](pic)_2$, as expected. The synthetic pathway for the tetracopper(II) complex may be represented by scheme 1.

The tetracopper(II) complex is insoluble in non-polar solvents and common polar solvents, but very soluble in DMF and DMSO to give stable solutions at room temperature. In the solid state, the tetracopper(II) complex is fairly stable in air allowing physical measurements. The molar conductance of the tetracopper(II) complex (98 S cm^2 M^{-1}) in DMF solution falls in the expected range for 1 : 2 electrolyte [33], suggesting that the tetracopper(II)

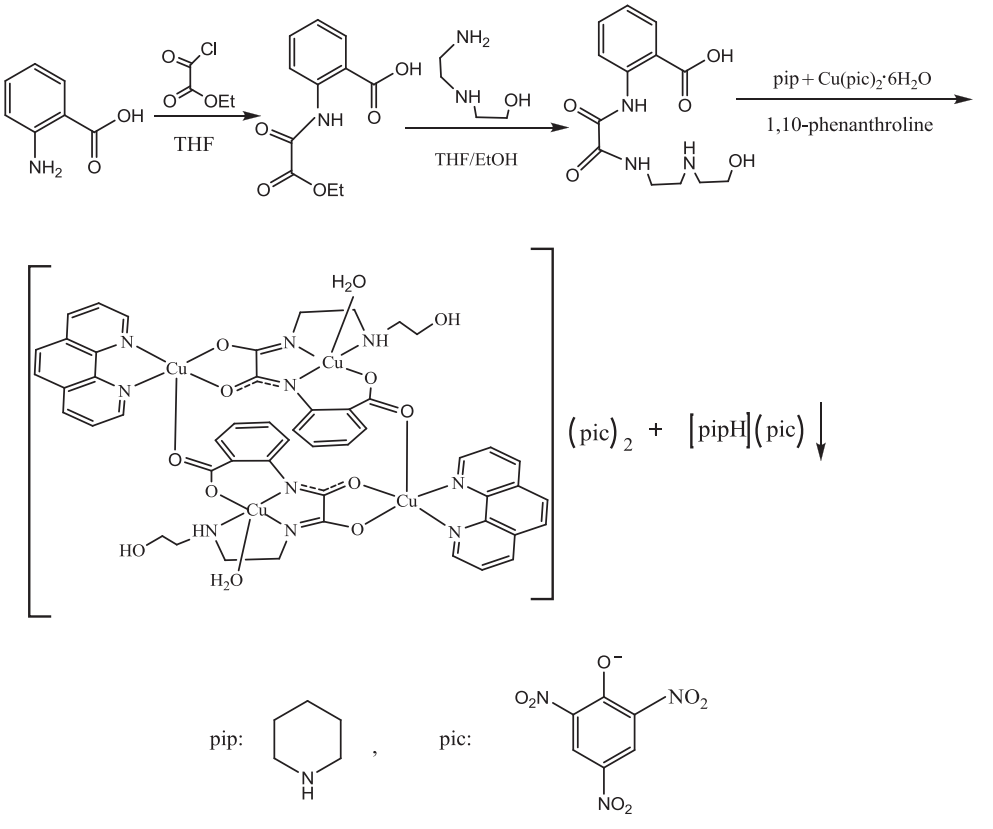

Scheme 1. The synthetic pathway for the tetracopper(II) complex.

complex consists of a tetracopper(II) cation $[Cu_4(bhyox)_2(phen)_2(H_2O)_2]^{2+}$ and two uncoordinated picrates in solution. The structure of the complex was further characterized by the following spectra and single crystal X-ray diffraction.

3.2. *IR spectra*

IR spectrum from 4000 to 400 cm^{-1} provides information regarding the mode of coordination in the tetracopper(II) complex in a careful comparison with that of the free H_3bhyox. The antisymmetric stretching vibration of carboxylate ν_{as}(COO), together with the carbonyl stretching vibration of oxamidate ν(C=O) of free H_3bhyox (1675 cm^{-1}) shifted to lower wavenumber of 1631 cm^{-1} in the IR spectrum of the complex (figure S1), implying that not only the carbonyl oxygens of oxamide but also the oxygens of carboxylate in the free bridging ligand coordinate with copper(II) to form tetracopper(II) complex [34]. This shift has often been used as a diagnostic indicator for oxamido-bridged structures [22]. The ν(C=N) stretching vibration for the terminal ligand (phen) at 1430 cm^{-1} indicates coordination of nitrogen of terminal ligands with copper(II) [35]. Free Hpic has $\nu_{as}(NO_2)$ at 1557 cm^{-1} and $\nu_s(NO_2)$ at 1342 cm^{-1}, respectively. However, in the tetracopper(II) complex, $\nu_{as}(NO_2)$ of pic^- emerges at 1560 cm^{-1} and $\nu_s(NO_2)$ of pic^- splits into two bands at 1360 and 1325 cm^{-1}, suggesting that the oxygens of pic–take no part in coordination [36]. This is consistent with the molar conductance value of the tetracopper(II) complex.

3.3. *Electronic spectra*

To obtain further structural information, the electronic spectrum of the tetracopper(II) complex was measured from 200 to 800 nm. Spectra obtained for the tetracopper(II) complex at different concentrations (1.7×10^{-4}–1.7×10^{-6} M) obeyed the Beer–Lambert law, indicating that the tetracopper(II) complex stays intact at these concentrations [37]. This is consistent with the molar conductance measurement. As shown in figure S2, for the tetracopper(II) complex, two main absorptions with varied intensities can be observed. The intense band at 230 nm is assignable to inter- or intra-ligand (π–π^*) transition, while the band at 272 nm in the tetracopper(II) complex can be assigned to the charge transfer transition between ligand and metal.

These spectroscopic data of the tetracopper(II) complex are supported by the determination of the crystal structure (*vide infra*).

3.4. *Structure description of $[Cu_4(bhyox)_2(phen)_2(H_2O)_2](pic)_2$*

There is one centrosymmetric tetracopper(II) complex in each unit cell. The asymmetric unit (ASU) consists of half of the complex, i.e. the ASU is centrosymmetrically related to the other half, and can be considered as a *cis*-oxamido-bridged bicopper(II) complex cation balanced by a picrate anion. As shown in figure 1, the two bicopper(II) cations head-to-tail bond via the carboxylate groups to form a cyclic system. The two Cu···Cu separations through the oxamido and the carboxylate bridges are 5.1944(6) and 5.3344(7) Å, respectively. The two "trans" Cu···Cu distances are 5.8783(8) (Cu1···Cu1^{i}) and 8.7361(9) (Cu2···Cu2^{i}) Å [symmetry code: (i) $1-x$, $-y$, $1-z$]; the former is not that much longer than the two Cu···Cu separations. The *cis*-oxamide group coordinates to Cu1 and Cu2 in the usual chelating mode [38, 39], with bite angles of 84.17(8)° and 85.15(7)°, respectively. The carboxylate group bridges copper(II) ions in a skew–skew fashion [40, 41] with torsion angles of Cu1–O1–C1–O2 [158.75(17)°] and Cu2^{i}–O2–C1–O1 [−106.3(2)°]. As a comparison, Cu···Cu distances *via* oxamide bridges [38, 39] and *via* carboxylates [25, 39, 40] are 5.198(1), 5.186(3), 5.3141, 5.225(4) and 5.2871(5) Å, respectively, similar Cu···Cu separations via oxamide bridge and carboxylate bridge with the present tetracopper(II) complex.

Both Cu1 and Cu2 have square–pyramidal coordination geometries with τ values of 0.03 and 0.16, respectively [42], displaced 0.1435(11) and 0.1986(10) Å from their basal planes, respectively. The five-membered ring (Cu1–N2–C10–C11–N3) of Cu1 chelating with ethylenediamine adopts a twist conformation with puckering parameters [43] of $Q = 0.438(3)$ Å and $\varphi = 300.6(3)°$. The other three five-membered chelating rings (Cu1–N1–C8–C9–N2, Cu2–O3–C8–C9–O4, and Cu2–N4–C25–C24–N5) are essentially planar. While the six-membered ring (Cu1–O1–C1–C2–C3–N1) has puckering parameters of Q [0.236(2) Å], θ [93.0(5)°], and φ [289.8(5)°], which implies a flattened boat conformation. The Cu1–N3 bond [2.080(2) Å] is longer than Cu1–N1 [1.9944(19) Å] and Cu1–N2 bond [1.906(2) Å], consistent with the stronger donor ability of deprotonated amido nitrogen compared with the amine [44]. Considering the average C–N distances [45] of –C(=O)NR_2 (1.346 Å), –C(=O)NHR (1.334 Å), and –C(=O)NH_2 (1.325 Å) decrease in succession due to the proportion of imidic acid forming in amide–imidic acid resonance structures, the shorter C8–N1 bond [1.305(3) Å] implies more imidic acid contribution. Besides, the Cu1–N1 bond length is close to Cu2–N4 and Cu2–N5. They both indicate that the amide of N1 is a delocalized

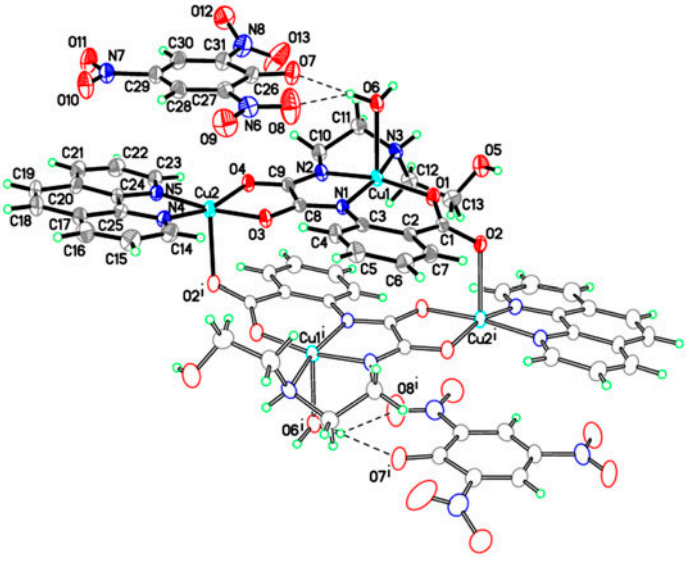

Figure 1. A view of the tetracopper(II) complex with the atom numbering scheme. Displacement ellipsoids are drawn at the 30% probability level and hydrogens are shown as small spheres of arbitrary radii. Dashed lines indicate hydrogen bonds [symmetry code: (i) $1-x, -y, 1-z$].

bond, that is to say, the amide and the imidic acid resonance conformation are comparable. As illustrated in scheme 2 and in the resonance structure for the oxamido bridge for the amide, the complex has formally a $Cu1^{1+}$ cation and a Cu2 neutral species. While for the imidic one, the formal charges at Cu1 and Cu2 are 0 and 1+, respectively. The Cu1–N2 bond is shorter by 0.08 Å than other Cu–N (sp^2 hybrid) bonds, suggesting different resonance structures on N1 and N2. Cu1–N2 and C9–N2 distances [1.279(3) Å] are very similar to those in many Schiff base copper(II) complexes [46–49]. Therefore, the imidic component may dominate the C9–N2 bond. N1 is a delocalized amide nitrogen while N2 is an imidic N. In an analogous complex, $\{[Cu(oxbe)(py)]_2Ni(py)_2\}\cdot 2DMF$ (where H_3oxbe is the dissymmetrical ligand N-benzoato-N′-(2-aminoethyl)oxamido) [50], the obvious differences of Cu–N distances (1.988 *versus* 1.912 Å) and C–N distances (1.332 *versus* 1.290 Å) are also observed. It is reasonable to attribute these differences to the various resonance structures. Further investigations on this and similar systems are required to get deeper insight into copper(II) complexes with *N*,*N*′-bis(substituted)oxamide bridging ligands.

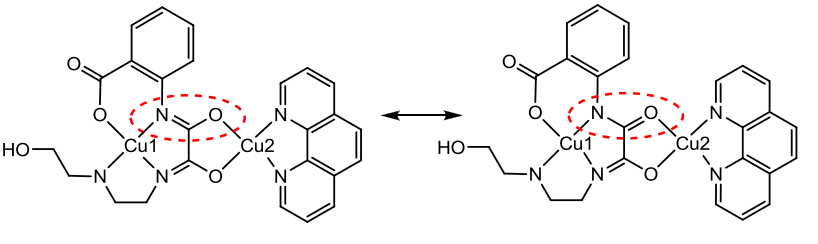

Scheme 2. The resonance structure of the μ-oxamido-bridge in the tetracopper(II) complex.

As shown in figure 2, the supramolecular structure in the crystal is dominated by hydrogen bonds and π–π stacking interactions. The complex cations employ hydrogen bonds O5–H5A···O6^{ii}, O6–H6B···O1^{ii}, and O6–H6B···O2^{ii} [symmetry code: (ii) $2-x$, $-y$, $1-z$] through coordinated water to form a chain parallel to the a axis (table 3), and the picrates join the chain with the hydrogen bonds. Then these chains are assembled by non-classical C–H···O hydrogen bonds. In fact, these complexes compose a 2-D network parallel to the $1\,1\,\bar{1}$) plane via these hydrogen bonds (figure 3). Between the two layers, there are π–π stacking interactions. The pyridine ring containing N4 has an angle of 5.57(13)° with the benzene ring of bhyox^{3-} at $1-x$, $1-y$, $1-z$ (iii), and the angle between the center-to-center vector and the normal of N4-pyridine ring is 39.97°. To the pyridine ring, the nearest separation is 3.336(4) Å (C5^{iii}).

Compared with our previously reported $[Cu_4(bhyox)_2(dabt)_2](ClO_4)_2$ (dabt denotes diaminobithiazole) [25], with the same bridging ligand and metal ion, the differences are the terminal ligands, counter anions, and coordination water. The present tetracopper(II) complex crystallized in triclinic, *P-1* space group, while the previous complex $[Cu_4(bhyox)_2(dabt)_2](ClO_4)_2$ was monoclinic, *C2/c*, in which the hydroxyl group of bhyox^{3-} ligand coordinated to a copper(II) ion due to the absence of water, changing the hydroxyl participating in hydrogen bonds. Besides the different numbers of oxygens as acceptors of hydrogen bonds, the picrate is distinguished by the planar shape from the spherical perchlorate. Terminal phen has more aromatic ring system than dabt. These all result in the different behaviors in supramolecular structure. These differences of the structure have also affected on the following properties.

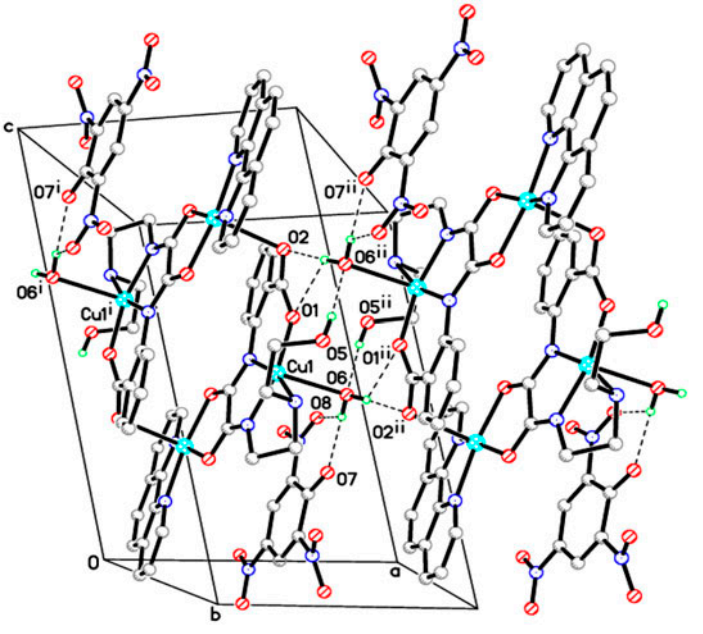

Figure 2. A view of the 1-D hydrogen-bonding structure parallel to the a axis. Symmetry codes: (i) $1-x$, $-y$, $1-z$; (ii) $2-x$, $-y$, $1-z$.

Table 3. Hydrogen-bonding geometries (Å, °) for the tetracopper(II) complex.

D–H···A	D–H	H···A	D···A	D–H···A
O5–H5A···O6^{ii}	0.822(10)	1.927(12)	2.742(3)	171(4)
O6–H6B···O1^{ii}	0.848(10)	2.53(3)	3.085(2)	124(3)
O6–H6B···O2^{ii}	0.848(10)	2.041(12)	2.883(3)	173(4)
O6–H6A···O7	0.850(10)	1.961(13)	2.791(3)	165(3)
O6–H6A···O8	0.850(10)	2.52(3)	3.061(3)	122(3)
C15–H15···O8^{iii}	0.93	2.56	3.482(4)	169.7
C16–H16···O5^{iv}	0.93	2.33	3.172(3)	150.0
C19–H19···O10^{v}	0.93	2.53	3.412(4)	157.7

Note: Symmetry codes: (ii) $2-x, -y, 1-z$; (iii) $1-x, 1-y, 1-z$; (iv) $x-1, y+1, z$; (v) $-x, 1-y, -z$.

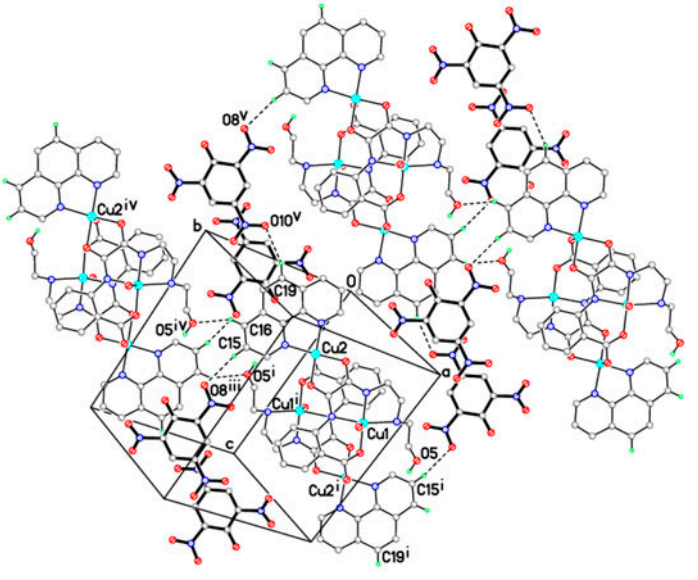

Figure 3. A view of the 2-D hydrogen-bonding structure parallel to $1\,1\,\bar{1}$ plane and a π–π stacking interaction between the two layers of the pyridine ring containing atom N4 and the benzene ring of bhyox^{3-} ligand. Symmetry codes: (i) $1-x, -y, 1-z$; (iii) $1-x, 1-y, 1-z$; (iv) $x-1, y+1, z$; (v) $-x, 1-y, -z$.

3.5. In vitro *antitumor activities of the tetracopper(II) complex*

In order to explore the potential antitumor activities of the tetracopper(II) complex, cytotoxicity assays of the tetracopper(II) complex and *cis*-platin against human hepatocellular carcinoma SMMC-7721 and human lung adenocarcinoma A549 were conducted. The IC_{50} values of the tetracopper(II) complex are 15.6 ± 0.3 and $19.2 \pm 0.5\,\mu M$ for SMMC-7721 and A549, respectively, which are lower than those of our previously reported analogous complex $[Cu_4(bhyox)_2(dabt)_2](ClO_4)_2$ [25], indicating that the present tetracopper(II) complex demonstrated better activities than the previously reported analogous complex. This may be partially attributed to its strong intercalation (*vide infra*). The IC_{50} values of the present tetracopper(II) complex are much higher than those of the clinically practiced antitumor drug *cis*-platin (IC_{50} values are 5.4 ± 0.2 and $7.6 \pm 0.4\,\mu M$

to these two kinds of cancer cell lines, respectively), suggesting that the cytotoxic activities of the present tetracopper(II) complex are less than that of *cis*-platin. However, the inhibition of cell proliferation produced by the present tetracopper(II) complex on the same batch of cell lines is still rather active. These findings of cytotoxic activities *in vitro* of the tetracopper(II) complex prompt us to explore the reactivities toward DNA and protein BSA.

3.6. *DNA interaction studies*

3.6.1. Electronic absorption titration. Electronic absorption spectroscopy is an effective method to examine the binding mode and magnitude of DNA with metal complexes. Hypochromism and red shift are associated with binding of metal complexes to the DNA helix, due to intercalation involving a strong stacking interaction between the aromatic chromophore of metal complexes and the base pairs of DNA [51]. Absorption spectra of the tetracopper(II) complex in the absence and presence of *HS*-DNA are depicted in figure 4. With incremental amounts of *HS*-DNA, the electronic spectrum exhibited hypochromism of about 14% at a ratio of 9 of the [DNA]/[complex], accompanied by slight bathochromic shift (3 nm) in the absorbance maxima. These spectral changes suggest that the tetracopper (II) complex interacts with *HS*-DNA through intercalation involving π–π stacking between the aromatic chromophore and the base pairs of DNA [52]. These observations for the tetracopper(II) complex are confirmed by the following observations. When the tetracopper (II) complex intercalates the base pairs of *HS*-DNA, the π^*-orbital of the intercalated phen in the tetracopper(II) complex can couple with the π-orbital of the base pairs, thus decreasing the π–π^* transition energy and resulting in bathochromism. Furthermore, the coupling π^*-orbital is partially filled by electrons, thereby decreasing the transition probabilities and concomitantly resulting in hypochromism.

In order to quantitatively evaluate the strength of the binding affinity of the tetracopper (II) complex toward *HS*-DNA, the intrinsic binding constant K_b of this tetracopper(II) complex with *HS*-DNA was determined by monitoring the changes in absorbance at 272 nm with increasing concentration of *HS*-DNA according to the following equation [53]:

$$[\mathrm{DNA}]/(\varepsilon_a - \varepsilon_f) = [\mathrm{DNA}]/(\varepsilon_b - \varepsilon_f) + 1/K_b(\varepsilon_b - \varepsilon_f) \quad (1)$$

where ε_a, ε_f, and ε_b correspond to the extinction coefficient, for each addition of *HS*-DNA to the tetracopper(II) complex, for the free tetracopper(II) complex, and for the tetracopper (II) complex in the fully bound form, respectively. As shown in figure 4 and in the plot of $[\mathrm{DNA}]/(\varepsilon_a - \varepsilon_f)$ *versus* [DNA], the binding constant K_b for the tetracopper(II) complex was $1.03 \times 10^5\,\mathrm{M}^{-1}$ ($R = 0.9996$ for six-points), lower than the classical intercalators (e.g. EB-DNA, $\sim 10^6\,\mathrm{M}^{-1}$) [54], but higher than those of some mono- and bicopper(II) complexes containing phen [55–57].

3.6.2. Fluorescence titration. To further verify the interaction mode between the tetracopper(II) complex and *HS*-DNA, EB fluorescence displacement assay was used. The intrinsic fluorescence intensity of DNA is very low and that of EB in Tris-HCl buffer is also not high due to quenching by solvent. However, on addition of DNA, the fluorescence intensity of EB is enhanced by intercalative binding to DNA. A competitive binding of the

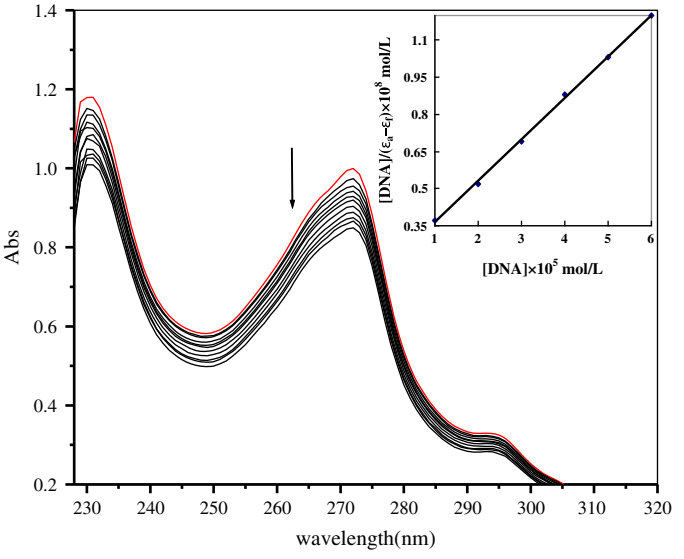

Figure 4. Absorption spectra of the tetracopper(II) complex upon titration of *HS*-DNA. Arrow indicates the change upon increasing DNA concentration. Inset: plot of [DNA]/($\varepsilon_a - \varepsilon_f$) *vs*. [DNA] for the absorption titration of *HS*-DNA with the tetracopper(II) complex.

metal complexes to *HS*-DNA can result in the reduction of the emission intensity due to the decreasing of the binding sites of DNA available for EB [58]. In our experiment (figure 5), the fluorescence intensity of EB bound to the DNA shows a remarkable decrease with increasing concentration of the tetracopper(II) complex at 584 nm, which indicates that some EB molecules were displaced from the EB–DNA system by the tetracopper(II) complex, resulting in fluorescence quenching of EB. The observation is considered as the characteristic of intercalation [59].

To understand quantitatively the magnitude of the binding strength of the tetracopper(II) complex with DNA, the classical linear Stern–Volmer equation is employed [60]:

$$I_0/I = 1 + K_{sv}[Q] \tag{2}$$

where I_0 and I represent the fluorescence intensities in the absence and presence of quencher, respectively, $[Q]$ is the concentration of quencher and K_{sv} is a linear Stern–Volmer quenching constant, given by the quenching plot of I_0/I *versus* [complex]. As shown in figure 5, the K_{sv} value for the tetracopper(II) complex is 1.73×10^5 ($R = 0.9971$ for eight-points).

Comparing with our previously reported analogous tetranuclear copper(II) complex $[Cu_4(bhyox)_2(dabt)_2](ClO_4)_2$ (K_b, $6.67 \times 10^4\,M^{-1}$; K_{sv}, 1.02×10^5) [25], the present tetracopper(II) complex $[Cu_4(bhyox)_2(phen)_2(H_2O)_2](pic)_2$ (K_b, $1.03 \times 10^5\,M^{-1}$; K_{sv}, 1.73×10^5) shows higher K_b and K_{sv} values, indicating that the present complex can strongly bind to the *HS*-DNA by intercalation. In fact, the two tetracopper(II) complexes have the same skeleton of $bhyox^{3-}$ bridging and metal ions, thus, their IR and electronic spectra are also similar. The main difference between them is their terminal ligands. The better binding affinity of the present complex to *HS*-DNA than that of the previously

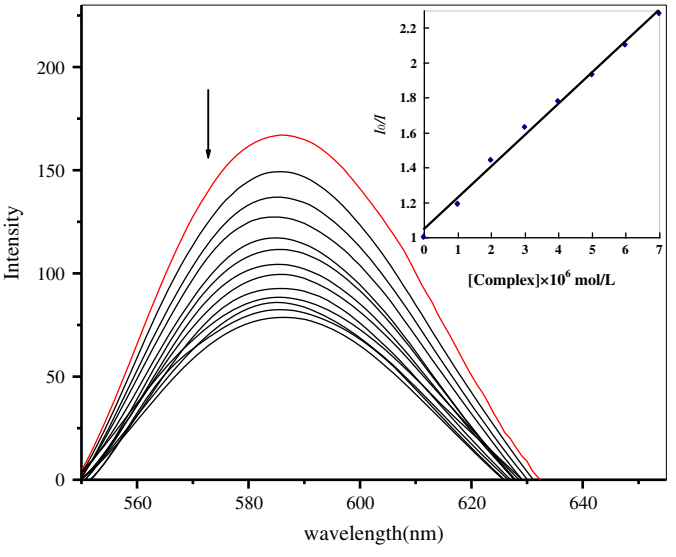

Figure 5. Emission spectra of *HS*-DNA–EB system upon titration of the tetracopper(II) complex. Arrow shows the change upon increasing complex concentration. Inset: plot of I_0/I *vs.* [complex] for the titration of tetracopper(II) complex to *HS*-DNA-EB system.

complex may be due to a more extended π-system of phen, which could intercalate better between the adjacent base pairs of DNA than that of dabt [61]. This suggests that different terminal ligands in such complexes have a profound effect on DNA-binding ability, as revealed by the different binding constants.

If we compare DNA-binding properties of the present tetracopper(II) complex with those of copper(II) complexes [39, 62–69] previously reported by us and other groups, modes and affinities of DNA binding of all these copper(II) complexes mainly depend on the nature of the ligands. Notably, in μ-oxamido-bridged polycopper(II) complexes, the interaction modes and DNA-binding ability may be tuned by changing the bridging or terminal ligands. Such strategy should be valuable in understanding the DNA-binding behaviors of this class of complexes as well as laying a foundation for the design of powerful agents for probing and targeting nucleic acids, providing insight into the field of DNA interactions.

3.6.3. Electrochemical titration. Cyclic voltammetry provides a useful complement to previously used spectral studies on the nature of DNA binding of the tetracopper(II) complex. Cyclic voltammograms of the tetracopper(II) complex are depicted in figure 6. In the absence of *HS*-DNA (red curve), the tetracopper(II) complex shows a couple of waves corresponding to Cu(II)/Cu(I) with cathodic (E_{pc}) and anodic peak potential (E_{pa}) being -0.248 and -0.122 V, respectively. The separation of anodic and cathodic peaks (ΔE_p) is 0.126 V, indicating quasi-reversible one-electron redox process ($I_{pc}/I_{pa} \approx 1$) in the tetracopper(II) complex. The formal potential of the Cu(I)/Cu(II) couple in free form ($E_f^{0\prime}$) taken as the average of E_{pc} and E_{pa} is -0.185 V. Upon addition of *HS*-DNA (blue curve) with $R = 5$ ($R = [\text{DNA}]/[\text{complex}]$), the voltammetric peak current decreased, indicating that interaction exists between the tetracopper(II) complex and *HS*-DNA [70]. Drop of the voltammetric current in the presence of *HS*-DNA may be attributed to slow diffusion of the tetracopper(II) complex

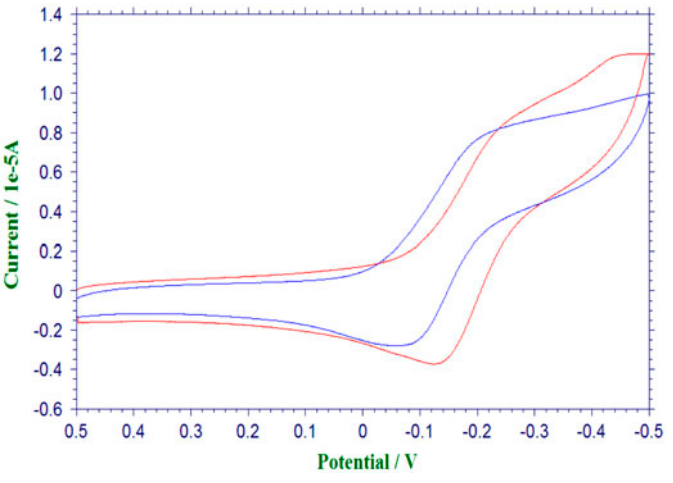

Figure 6. Cyclic voltammograms of the tetracopper(II) complex in the absence (red line) and presence (blue line) of *HS*-DNA (see http://dx.doi.org/10.1080/00958972.2013.827179 for color version).

bound to *HS*-DNA. The cathodic and anodic peak potentials are at −0.2116 and −0.0904 V, respectively. The peak-to-peak separation becomes larger with $\Delta E_p = 0.1212$ V, suggesting that in the presence of *HS*-DNA the electron-transfer process seems to become less reversible for the tetracopper(II) complex. The corresponding formal potential of the Cu(I)/Cu(II) couple in binding form ($E_b^{0\prime}$) is −0.151 V. The ($E_b^{0\prime}$) value of the tetracopper(II) complex is shifted to positive by 0.034 V, suggesting that the tetracopper(II) complex could bind intercalatively to *HS*-DNA [71], in agreement with the above spectral observations. The separation between $E_b^{0\prime}$ and $E_f^{0\prime}$ can be used to estimate the ratio of binding constants for the reduced and oxidized forms to DNA using the equation [72]:

$$E_b^{0\prime} - E_f^{0\prime} = 0.059 \log[K_{Cu(I)}/K_{Cu(II)}] \quad (3)$$

where $K_{Cu(I)}$ and $K_{Cu(II)}$ are the binding constants of Cu(I) and Cu(II) forms to DNA, respectively. The ratio of constants for the binding of Cu(I) and Cu(II) to *HS*-DNA was estimated to be 3.77 for the tetracopper(II) complex, suggesting that the reduced form of the tetracopper(II) complex interacts more strongly than the oxidized one. Thus, the electrochemical results are in agreement with the spectral studies, reinforcing the conclusion that the tetracopper(II) complex binds to *HS*-DNA in an intercalation mode.

3.6.4. Viscosity measurements. Viscosity measurement is sensitive to the change in length of DNA, regarded as the least ambiguous and the most critical means of studying the binding mode of metal complexes with DNA in solution, and provides strong arguments for intercalative-binding mode [30]. In classical intercalation the DNA helix lengthens as base pairs are separated to accommodate the bound ligand leading to an increased DNA viscosity; whereas in groove binding and electrostatic modes, the length of the helix is unchanged with no apparent alteration in DNA viscosity. The effects of the tetracopper(II) complex on the viscosity of *HS*-DNA are shown in figure 7. As illustrated in this figure, with increasing concentration of the tetracopper(II) complex the relative viscosity of *HS*-

DNA increases steadily, proving that tetracopper(II) complex binds to *HS*-DNA by intercalation [73]. Thus, the results of viscosity studies further validate those obtained from electronic absorption titration, fluorescence titration, and electrochemical titration.

The most direct evidence for the actual binding of the DNA with the tetracopper(II) complex might come from X-ray crystallographic studies. Unfortunately, all our efforts to grow crystals of the system for the tetracopper(II) complex intercalating into *HS*-DNA suitable for X-ray structure determination have been unsuccessful. However, based on the above discussion of the electronic absorption titration, EB fluorescence displacement experiment, electrochemical titration, and viscometry measurement, one can conclude that the intercalation is the most probable binding mode between the tetracopper(II) complex and *HS*-DNA. Further investigations by using other methods to get a reasonable explanation and deeper insight into the DNA-binding mode of the complex are in progress.

3.7. *BSA-binding properties*

3.7.1. Tryptophan quenching experiment. To examine protein binding behavior of the tetracopper(II) complex, tryptophan emission-quenching experiments were carried out using BSA as protein model due to its low cost, ready availability, and unusual ligand-binding properties. In general, changes in molecular environment in the vicinity of a fluorophore can be accessed by the changes in fluorescence spectra in the absence and presence of quencher and hence, provide clues for the nature of the binding phenomenon. The intrinsic fluorescence intensity of BSA comes from the two tryptophan side chains [74], Trp-134 and Trp-212, more exposed to the environment. Quenching can occur by different mechanisms, which are usually classified as dynamic quenching and static quenching. Dynamic quenching refers to a process in which the fluorophore and the quencher come into contact during the transient existence of the exited state. While static quenching is due to the formation of ground-state complex between the fluorophore and quencher. In both cases, the fluorescence intensity is related to the concentration of the quencher. Therefore, the quenched fluorophore can serve as an indicator for the quenching agent.

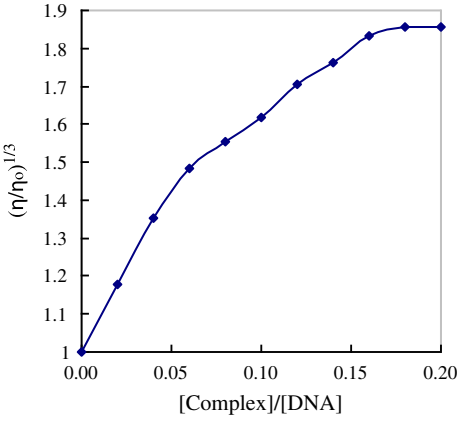

Figure 7. Effect of increasing amount of the tetracopper(II) complex on the relative viscosity of *HS*-DNA at 289 (±0.1) K, [DNA] = 0.1 mM.

The interaction of the tetracopper(II) complex with BSA protein was studied by fluorescence measurement at room temperature, and the results are illustrated in figure 8. BSA has a strong fluorescence emission peak at 278 nm. When BSA was titrated with different amounts of the tetracopper(II) complex, a remarkable intrinsic fluorescence decrease in BSA was observed, indicating that the interaction of the tetracopper(II) complex with BSA causes conformational changes in protein structure leading to changes in tryptophan microenvironment of BSA [75].

To understand quantitatively the magnitude of the tetracopper(II) complex to quench the emission intensity of BSA, the linear Stern–Volmer equation (4) is used:

$$I_0/I = 1 + K_{sv}[Q] = 1 + k_q\tau_0[Q] \tag{4}$$

where I_0 and I represent the fluorescence intensities in the absence and presence of quencher, respectively, Q is the concentration of quencher, K_{sv} is a linear Stern–Volmer quenching constant, k_q is the biomolecular quenching rate constant and τ_0 is the average lifetime of the fluorophore in absence of the quencher as 10^{-8} s. From the quenching plot of I_0/I *versus* [complex] (inset in figure 8), K_{sv} and k_q of the tetracopper(II) complex are $1.77 \times 10^5\,M^{-1}$ and $1.77 \times 10^{13}\,M^{-1}\,s^{-1}$ ($R = 0.9970$ for nine-points), respectively. However, maximum collision quenching constant of various kinds of quenchers to biomacromolecule is $2.0 \times 10^{10}\,M^{-1}\,s^{-1}$ [76]. Obviously, the rate of protein quenching initiated by the tetracopper(II) complex is greater than $2.0 \times 10^{10}\,M^{-1}\,s^{-1}$, indicating that above quenching is not initiated by dynamic collision but *via* the combination of the tetracopper (II) complex and BSA. In other words, the tetracopper(II) complex binds to BSA responsible for quenching of tryptophan fluorescence by static quenching mechanism [77]; this

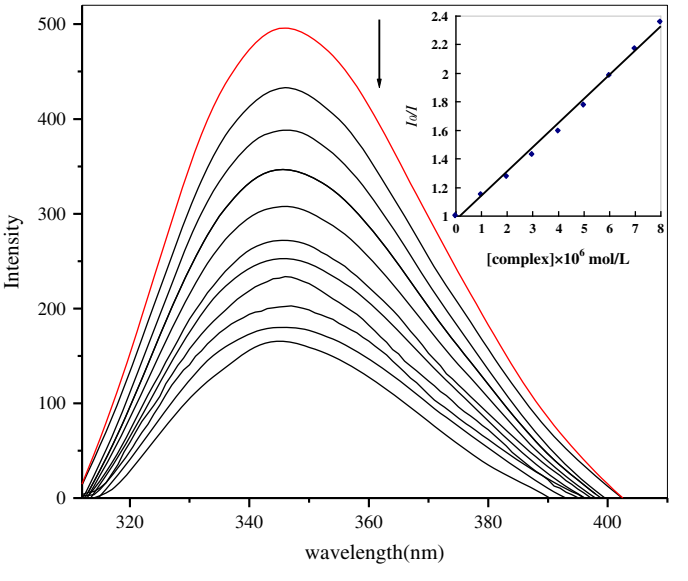

Figure 8. Emission spectra of BSA upon titration of the tetracopper(II) complex. Arrow shows the change upon increasing complex concentration. Inset: plot of I_0/I *vs.* [complex] for titration of the tetracopper(II) complex to BSA.

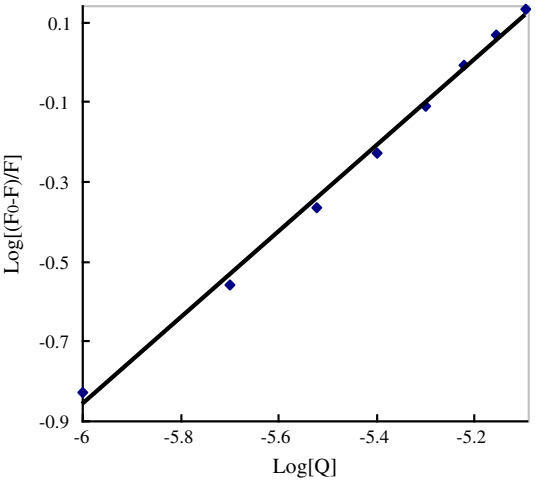

Figure 9. Plot of $\log[(F_0-F)/F]$ *vs.* $\log[Q]$ for the titration of the tetracopper(II) complex to BSA.

viewpoint was also validated by the following UV absorption spectra studies. The binding constant (K) was calculated by the method given in the following section.

3.7.2. Binding constant and number of binding sites. On small molecules binding independently to a set of equivalent sites on a macromolecule, the equilibrium between the free and the bound molecule is given by the following equation [78, 79]:

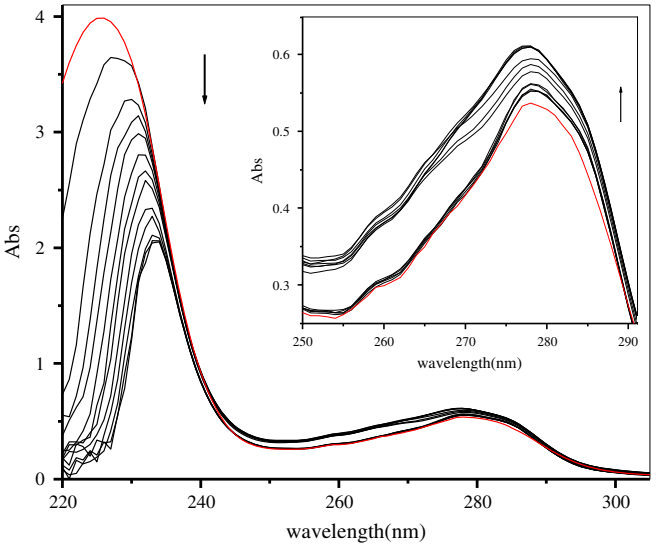

Figure 10. Absorption spectra of BSA upon titration of the tetracopper(II) complex. Arrow indicates the change upon increasing complex concentration.

$$\log[(F_0 - F)/F] = \log K + n \log[Q] \quad (5)$$

where F_0 and F represent the fluorescence intensities in the absence and presence of quencher, respectively, K is the binding constant of the tetracopper(II) complex with BSA and n is the number of binding sites. From the quenching plot of $\log[(F_0-F)/F]$ *versus* $\log[Q]$ (figure 9), K and n of the tetracopper(II) complex can be obtained. The K and n values are 4.18×10^5 ($R = 0.9979$ for eight-points) and 1.08, respectively. The binding sites n is about 1, indicating that there is just one binding site in BSA for the tetracopper(II) complex.

3.7.3. UV absorption spectral studies. UV–visible absorption spectroscopy is a simple method to explore the type of quenching [80]. To confirm the probable quenching mechanism of the tetracopper(II) complex, UV absorption spectroscopy was employed. The UV absorption spectra of BSA in the absence and presence of different concentrations of the tetracopper(II) complex are shown in figure 10. The absorption intensity of BSA was enhanced with addition of the tetracopper(II) complex and accompanied by a little blue shift. This indicates that there exists a static interaction between BSA and the tetracopper (II) complex due to the formation of ground-state complex of the type BSA-compound as reported earlier [80], which is in agreement with the observation derived by the tryptophan emission-quenching studies.

Thus, the results observed in fluorescence and UV spectra measurements confirm the effective binding of the tetracopper(II) complex with BSA, and quenching is static quenching.

4. Conclusions

To investigate the influence of structural variation of the terminal ligands in tetracopper(II) complexes on structure, DNA- and protein-binding properties, as well as cytotoxic activities, a new tetracopper(II) complex, $[Cu_4(bhyox)_2(phen)_2(H_2O)_2](pic)_2$, has been synthesized and structurally characterized by single-crystal X-ray diffraction. The reactivity towards *HS*-DNA and BSA reveal that the tetracopper(II) complex interacts with *HS*-DNA by intercalation, and the complex binds to BSA responsible for quenching of tryptophan fluorescence by static quenching mechanism. *In vitro* cytotoxic activities suggest that the tetracopper(II) complex is active against selected tumor cell lines. Comparing the DNA-binding properties and *in vitro* anticancer activities with another tetracopper(II) complex with similar structure, it is obvious that the terminal ligands in these tetranuclear systems influence the structure and DNA-binding ability. Activities of these tetracopper(II) complexes to cancer cell lines are in accord with their DNA-binding abilities, suggesting that the cytotoxic activities of these tetracopper(II) complexes may be associated with or originate from their ability to intercalate the base pairs of DNA. The present investigation attest that varying terminal ligands in tetranuclear systems can create interesting differences in the configuration and electron density distribution, which result in differences in DNA- and BSA-binding behaviors and cytotoxic activities. Affinity magnitudes toward *HS*-DNA and BSA, and cytotoxic activities may be controlled by the nature of the terminal ligands in tetranuclear complexes. This strategy should be valuable in understanding the DNA- and protein-binding properties of the tetranuclear complexes as well as laying a foundation for the design of powerful agents for probing and targeting nucleic acids and proteins. Further investigations using various terminal ligands are still required to confirm this effect.

Supplementary material

CCDC 917220 contains the supplementary crystallographic data for this paper. Copies of this information can be obtained for free from The Director, CCDC, 12 Union Road, Cambridge, CB2 1EZ, UK (Fax: C44 1233 336 033; E-mail: deposit@ccdc.cam.ac.uk).

Acknowledgments

This project was supported by the National Natural Science Foundation of China (Nos. 21071133, 51273184 and 81202399), the Program for Science and Technology of Shandong Province (No. 2011GHY11521), and the Natural Science Foundation of Qingdao City [Nos. 11-2-4-1-(9)gch), 12-1-3-52-(1)-nsh and 12-1-4-16-(7)-jch].

References

[1] M. Chauhan, K. Banerjee, F. Arjmand. *Inorg. Chem.*, **46**, 3072 (2007).
[2] F. Arjmand, M. Aziz. *Eur. J. Med. Chem.*, **44**, 834 (2009).
[3] M.J. Clarke. *Coord. Chem. Rev.*, **236**, 209 (2003).
[4] E. Wong, C.M. Giandomenico. *Chem. Rev.*, **99**, 2451 (1999).
[5] L. Ronconi, P.J. Sadler. *Coord. Chem. Rev.*, **251**, 1633 (2007).
[6] S.E. Sherman, D. Gibson, A.H.J. Wang, S.J. Lippard. *J. Am. Chem. Soc.*, **110**, 7368 (1988).
[7] P.M. Takahara, C.A. Frederick, S.J. Lippard. *J. Am. Chem. Soc.*, **118**, 2309 (1996).
[8] A. Panja. *Polyhedron*, **43**, 22 (2012).
[9] U. Pindur, M. Haber, K. Sattler. *J. Chem. Educ.*, **70**, 263 (1993).
[10] H. Malonga, J.F. Neault, H.A. Tajmir-Riahi. *DNA Cell Biol.*, **25**, 393 (2006).
[11] H. Gao, Y.N. Wang, Y.G. Fan, J.B. Ma. *Bioorg. Med. Chem.*, **14**, 131 (2006).
[12] A. Silvestri, G. Barone, G. Ruisi, M.T. Giudice, S. Tumminello. *J. Inorg. Biochem.*, **98**, 589 (2004).
[13] K.D. Karlin, Z. Tyeklar. *Bioinorganic Chemistry of Copper*, Chapman & Hill, New York (1993).
[14] R.E. Holmlin, E.D.K. Stemp, J.K. Barton. *Inorg. Chem.*, **37**, 29 (1998).
[15] S. Dhar, D. Senapati, P.K. Das, P. Chattopadhyay, M. Nethaji, A.R. Chakravarty. *J. Am. Chem. Soc.*, **125**, 12118 (2003).
[16] D.S. Sigman, D.R. Graham, V.D. Aurora, A.M. Stern. *J. Biol. Chem.*, **254**, 12269 (1979).
[17] R. Ren, P. Yang, W.J. Zheng, Z.C. Hua. *Inorg. Chem.*, **39**, 5454 (2000).
[18] K. Dhara, P. Roy, J. Rarha, M. Manassero, P. Banerjee. *Polyhedron*, **26**, 4509 (2007).
[19] A. Dimitrakopoulou, C. Dendrinou-Samara, A.A. Pantazaki, M. Alexiou, E. Nordlander, D.P. Kessissoglou. *J. Inorg. Biochem.*, **102**, 618 (2008).
[20] R. Tang, C.H. Tang, C.Q. Tang. *J. Organomet. Chem.*, **696**, 2040 (2011).
[21] E.G. Ferrer, A. Bosch, O. Yantorno, E.J. Baran. *Bioorg. Med. Chem.*, **16**, 3878 (2008).
[22] H. Ojima, K. Nonoyama. *Coord. Chem. Rev.*, **92**, 85 (1988).
[23] R. Ruiz, J. Faus, F. Lloret, M. Julve, Y. Journaux. *Coord. Chem. Rev.*, **193–195**, 1069 (1999).
[24] X.W. Li, Y. Yu, Y.T. Li, Z.Y. Wu, C.W. Yan. *Inorg. Chim. Acta*, **367**, 64 (2011).
[25] W.C. Chen, L.D. Wang, Y.T. Li, Z.Y. Wu, C.W. Yan. *Transition Met. Chem.*, **37**, 569 (2012).
[26] G.M. Sheldrick. *SHELXL97, Program for Crystal Structure Refinement,* University of Göttingen, Germany (1997).
[27] J. Marmur. *J. Mol. Biol.*, **3**, 208 (1961).
[28] M.E. Reichmann, S.A. Rice, C.A. Thomas, P.J. Doty. *J. Am. Chem. Soc.*, **76**, 3047 (1954).
[29] J.B. Chaires, N. Dattagupta, D.M. Crothers. *Biochemistry*, **21**, 3933 (1982).
[30] G. Cohen, H. Eisenberg. *Biopolymers*, **8**, 45 (1969).
[31] J.K. Barton, J.M. Goldberg, C.V. Kumar, N.J. Turro. *J. Am. Chem. Soc.*, **108**, 2081 (1986).
[32] N.S. Quiming, R.B. Vergel, M.G. Nicolas, J.A. Villanueva. *J. Health Sci.*, **51**, 8 (2005).
[33] W.J. Geary. *Coord. Chem. Rev.*, **7**, 81 (1971).
[34] Y.Y. Gu, Y.T. Li, Z.Y. Wu, W. Sun, M. Jiang. *Acta Crystallogr., Sect. C*, **C65**, 115 (2009).
[35] K. Nakamoto. *Infrared and Raman Spectra of Inorganic and Coordination Compounds*, 5th Edn , Wiley, New York (1997).
[36] S.X. Liu, W.S. Liu, M.Y. Tan, K.B. Yu. *J. Coord. Chem.*, **39**, 105 (1996).
[37] A.B.P. Lever. *Inorganic Electronic Spectroscopy*, Elsevier Science Publishers BV, Amsterdam (1984).
[38] Y. Journaux, J. Sletten, O. Kahn. *Inorg. Chem.*, **25**, 439 (1986).

[39] X.W. Li, M. Jiang, Y.T. Li, Z.Y. Wu, C.W. Yan. *J. Coord. Chem.*, **63**, 1582 (2010).
[40] X.W. Li, Y.T. Li, Z.Y. Wu, F.B. Jiang. *Acta Crystallogr., Sect. C*, **C66**, 218 (2010).
[41] L.M. Duan, F.T. Xie, X.Y. Chen, Y. Chen, Y.K. Lu, P. Cheng, J.Q. Xu. *Cryst. Growth Des.*, **6**, 1101 (2006).
[42] A.W. Addison, T.N. Rao, J. Reedijk, J. Van Rijin, G.C. Verschoor. *J. Chem. Soc., Dalton Trans.*, 1349 (1984).
[43] D. Cremer, J.A. Pople. *J. Am. Chem. Soc.*, **97**, 1354 (1975).
[44] M. Baldini, M. Belicchi-Ferrari, F. Bisceglie, P.P. Dall' Aglio, G. Pelosi, S. Pinelli, P. Tarasconi. *Inorg. Chem.*, **43**, 7170 (2004).
[45] F.H. Allen, D.G. Watson, L. Brammer, A.G. Orpen, R. Taylor. *International Tables for Crystallography,* Vol. C, Chap. 9.5, 790–811 Springer-Verlag, Berlin (2004).
[46] J.M. Epstein, B.N. Figgis, A.H. White, A.C. Willis. *J. Chem. Soc., Dalton Trans.*, 1954 (1974).
[47] M.F. Iskander, T.E. Khalil, W. Haase, R. Werner, I. Svoboda, H. Fuess. *Polyhedron*, **20**, 2787 (2001).
[48] S. Das, S. Pal. *J. Mol. Struct.*, **753**, 68 (2005).
[49] P.K. Nanda, G. Aromi, D. Ray. *Inorg. Chem.*, **45**, 3143 (2006).
[50] R.J. Tao, S.Q. Zang, Q.L. Wang, Y.X. Cheng, J.Y. Niu, D.Z. Liao. *J. Coord. Chem.*, **57**, 947 (2004).
[51] V.A. Bloomfield, D.M. Crothers, I. Tinoco. *Physical Chemistry of Nucleic Acids,* p. 432, Harper and Row, New York (1974).
[52] S. Mahadevan, M. Palaniandaver. *Inorg. Chem.*, **37**, 693 (1998).
[53] S.E. Evans, M.A. Mendez, K.B. Turner, L.R. Keating, R.T. Grimes, S. Melchoir, V.A. Szalai. *J. Biol. Inorg. Chem.*, **12**, 1235 (2007).
[54] M. Sunita, M. Padmaja, B. Anupama, C. Gyana Kumari. *J. Fluoresc.*, **22**, 1003 (2012).
[55] T. Gupta, S. Dhar, M. Nethaji, A.R. Chakravarty. *J. Chem. Soc., Dalton Trans.*, 1896 (2004).
[56] R. Rao, A.K. Patra, P.R. Chetana. *Polyhedron*, **27**, 1343 (2008).
[57] J.Z. Wu, L. Yuan, J.F. Wu. *J. Inorg. Biochem.*, **99**, 2211 (2005).
[58] K. Dhara, P. Roy, J. Ratha, M. Manassero, P. Banerjee. *Polyhedron*, **26**, 4509 (2007).
[59] S. Anbu, M. Kandaswamy, P. Suthakaran, V. Murugan, B. Varghese. *J. Inorg. Biochem.*, **103**, 401 (2009).
[60] O. Stern, M. Volmer. *Z. Phys.*, **20**, 183 (1919).
[61] X.W. Li, Y.J. Zheng, Y.T. Li, Z.Y. Wu, C.W. Yan. *Eur. J. Med. Chem.*, **46**, 3851 (2011).
[62] Y.J. Zheng, X.W. Li, Y.T. Li, Z.Y. Wu, C.W. Yan. *J. Coord. Chem.*, **65**, 3530 (2012).
[63] M. Jiang, Y.T. Li, Z.Y. Wu. *J. Coord. Chem.*, **65**, 1858 (2012).
[64] S.H. Cui, M. Jiang, Y.T. Li, Z.Y. Wu, X.W. Li. *J. Coord. Chem.*, **64**, 4209 (2012).
[65] H.H. Lu, Y.T. Li, Z.Y. Wu, K. Zheng, C.W. Yan. *J. Coord. Chem.*, **64**, 1360 (2011).
[66] X.W. Zhang, Y.J. Zheng, Y.T. Li, Z.Y. Wu, C.W. Yan. *J. Coord. Chem.*, **63**, 2985 (2010).
[67] H.L. Wu, X.C. Huang, B. Liu, F. Kou, F. Jia, J.K. Yuan, Y. Bai. *J. Coord. Chem.*, **64**, 4383 (2011).
[68] Y. Mei, J.J. Zhou, H. Zhou, Z.Q. Pan. *J. Coord. Chem.*, **65**, 643 (2012).
[69] L.H. Zhi, W.N. Wu, Y. Wang, G. Sun. *J. Coord. Chem.*, **66**, 227 (2013).
[70] Y.M. Song, P.J. Yang, M.L. Yang, J.W. Kang, S.Q. Qin, B.Q. Lü. *Transition Met. Chem.*, **28**, 712 (2003).
[71] M.T. Carter, M. Rodriguez, A.J. Bard. *J. Am. Chem. Soc.*, **111**, 8901 (1989).
[72] L. Jin, P. Yang. *J. Inorg. Biochem.*, **68**, 79 (1997).
[73] M. Jiang, Y.T. Li, Z.Y. Wu, Z.Q. Liu, C.W. Yan. *J. Inorg. Biochem.*, **103**, 833 (2009).
[74] B.F. Pan, F. Gao, L.M. Ao. *J. Magn. Magn. Mater.*, **293**, 252 (2005).
[75] S.S. Bhat, A.A. Kumbhar, H. Heptullah, A.A. Khan, V.V. Gobre, S.P. Gejji, V.G. Puranik. *Inorg. Chem.*, **50**, 545 (2011).
[76] W.R. Ware. *J. Phys. Chem.*, **66**, 455 (1962).
[77] D.J. Li, M. Zhu, C. Xu, B.M. Ji. *Eur. J. Med. Chem.*, **46**, 588 (2011).
[78] V. Anbazhagan, R. Renganathan. *J. Lumin.*, **128**, 1454 (2008).
[79] P. Banerjee, S. Ghosh, A. Sarkar, S.C. Bhattacharya. *J. Lumin.*, **131**, 316 (2011).
[80] D.S. Raja, N.S.P. Bhuvanesh, K. Natarajan. *Eur. J. Med. Chem.*, **47**, 73 (2012).